



Journal of the Serbian *el*ectronic Chemical Society

JSCS-info@shd.org.rs • www.shd.org.rs/JSCS

ACCEPTED MANUSCRIPT

This is an early electronic version of an as-received manuscript that has been accepted for publication in the Journal of the Serbian Chemical Society but has not yet been subjected to the editing process and publishing procedure applied by the JSCS Editorial Office.

Please cite this article as H. Li, L. Ma, Z. Wu, and C. Yao, *J. Serb. Chem. Soc.* (2026) <https://doi.org/10.2298/JSC251115005L>

This “raw” version of the manuscript is being provided to the authors and readers for their technical service. It must be stressed that the manuscript still has to be subjected to copyediting, typesetting, English grammar and syntax corrections, professional editing and authors’ review of the galley proof before it is published in its final form. Please note that during these publishing processes, many errors may emerge which could affect the final content of the manuscript and all legal disclaimers applied according to the policies of the Journal.



Enhanced photocatalytic performance of ZnO/Cu₂O composite for the degradation of methylene blue under the synergy effect

HONGYING LI^{1,2}, LUWEN MA¹, ZHENYANG WU¹, AND CHENGLI YAO^{1*}

¹*School of Chemistry and Pharmaceutical Engineering, Hefei Normal University, Hefei, Anhui, China, and ²Hefei National Research Center for Physical Sciences at the Microscale, University of Science and Technology of China, Hefei, Anhui, China.*

(Received 15 November 2025; revised 27 November 2025; accepted 29 January 2026)

Abstract: In order to investigate the catalytic degradation efficiency of ZnO/Cu₂O composite, the nanocomposite was synthesized via one-pot method and the template of SDS. The crystal structure, microscopic morphology, chemical composition, specific surface area, pore size distribution and optical absorption property of the composite were characterized. Under the irradiation of xenon lamp, the photocatalytic performance of the composite was evaluated by degrading methylene blue (MB). The aforementioned characterization determined that the synthesized composite consisted of ZnO (hexagonal wurtzite) and Cu₂O (cubic crystal). Due to the mediation of SDS template, the particles were nanoscale with uniform distribution of Cu, Zn, and O elements and contained abundant mesopores. The photo-response range of the composite expanded to the visible region because of the combination of ZnO and Cu₂O. Degradation ratio of MB catalyzed by ZnO/Cu₂O maintained about 92% within 100 minutes after five recycling, demonstrating promising potentiality for photocatalytic applications. The enhanced photocatalytic performance maybe related to the mediation of SDS during the preparation process and the synergy effect between ZnO and Cu₂O.

Keywords: SDS; template; ZnO/Cu₂O; photocatalytic degradation.

INTRODUCTION

In recent years, wastewater pollution has got increasingly serious with the rapid development of industrialization. Dyes, pesticides, antibiotics, and other organic pollutants which are difficult to degrade in wastewater seriously threaten the safety of water ecosystem and human health. Photocatalytic degradation, as a high-efficiency and environment-friendly wastewater treatment technology, has attracted much attention in recent years.¹⁻⁴ ZnO,⁵⁻⁶ CdS,⁷ WO₃,⁸ TiO₂,⁹ Cu₂O,¹⁰ SnO₂,¹¹ and so on, have once been selected as semiconductor photocatalysts to

* Corresponding author. E-mail: yaochengli@hfnu.edu.cn
<https://doi.org/10.2298/JSC251115005L>

degrade organic pollutants in wastewater, however, the photocatalytic performance of a single catalyst is not high. Taking Cu₂O as an example, as a p-type semiconductor with a narrow band gap (E_g=2.1 eV), it was once considered as a potential photocatalyst because of its low price, environmental friendliness and absorption of most visible light.¹⁰ However, the electron-hole pairs generated in Cu₂O after absorbing light energy were easy to recombine quickly. Moreover, Cu₂O was easy to be oxidized in humid environment, so its photocatalytic performance was unsatisfactory.¹² To improve the photocatalytic performance of Cu₂O, the deposition of metals,¹² doping of nonmetallic elements,¹³ recombination with other materials,¹⁴ or construction of heterojunction¹⁵ was selected.

As an n-type semiconductor with wide band gap (E_g=3.37 eV), ZnO has attracted significant attention in recent years by virtue of good chemical stability, convenient preparation method, non-toxicity and low price.^{5-6, 16} However, as a photocatalyst, ZnO can only be excited by ultraviolet light with high energy, which results in the low utilization efficiency for sunlight and limits its wide application in photocatalytic field. Relevant literatures suggested that the photocatalytic property of the composite through combining ZnO with Cu₂O was improved significantly. On one hand, the absorption spectrum of the composite declared a red shift, which significantly improved the availability of sunlight. On the other hand, the separation of photo-generated e⁻ and h⁺ was effectively promoted due to the energy level matching of two semiconductor materials.¹⁷⁻¹⁸

Surfactants were often used as soft templates to effectively control the morphology and enhance the dispersibility of materials.¹⁹⁻²⁰ Up to now, the preparation and photocatalytic performance of ZnO/Cu₂O composite have been studied,^{17-18, 21-23} but it is rarely reported that surfactants are used as templates to regulate the formation of ZnO/Cu₂O. So, it is worthy of exploring sodium dodecyl sulfate (SDS) mediating the morphology and structure of ZnO/Cu₂O as well as its properties. Here, ZnO/Cu₂O composite was prepared via one-pot method with the template of SDS. The molecules of SDS self-assembled to form ordered aggregates with specific structures, its hydrophilic groups attracted metal ions, thereby changed the distribution of metal ions in the reaction system. Due to the mediation of SDS template, the composite composed of flower-like nano ZnO and Cu₂O nanospheres was prepared, which exhibited satisfactory photocatalytic degradation performance of MB under simulated sunlight. This provided a facile way for the preparation of economical and efficient photocatalysts for wastewater treatment.

EXPERIMENTAL

Chemicals

Sodium hydroxide (NaOH, AR), glucose (C₆H₁₂O₆, AR), sodium dodecyl sulfate (SDS) (C₁₂H₂₅SO₄Na, AR), zinc acetate dihydrate (Zn(CH₃COO)₂·2H₂O, AR), copper acetate monohydrate (Cu(CH₃COO)₂·H₂O, AR), methylene blue (C₁₆H₁₈N₃ClS, AR), and absolute ethanol (C₂H₅OH, AR). Deionized water was used in the whole experiment.

Preparation of ZnO/Cu₂O with SDS as a template

1.5g SDS was added into a beaker containing the mixed solution of Zn(CH₃COO)₂ (0.5 mol/L, 50 mL), Cu(CH₃COO)₂ (0.5 mol/L, 50 mL), and glucose (1 mol/L, 25 mL). The beaker was placed in a water bath (60 °C) and kept magnetic stirring for 30 min. Later, NaOH solution (2 mol/L, 50 mL) was added into it drop by drop. The mixing process was assisted by magnetic stirring and lasted for 30 min. The sediment at the bottom of the beaker was collected by centrifugation. It was washed alternately by water and ethanol three times each, and dried under vacuum at 60 °C. The desired sample was prepared and named as S1.

Preparation of ZnO/Cu₂O, ZnO, and Cu₂O

For comparison, ZnO/Cu₂O, ZnO, and Cu₂O without SDS were also synthesized. The following procedure described the synthesis steps. The preparation of ZnO/Cu₂O composite without SDS mediating was similar as S1, except that SDS was not added. The obtained sample was labeled as S2. 50 mL of Zn(CH₃COO)₂ solution (0.5 mol/L) was placed in the water bath (60 °C). Then 25 mL of NaOH solution (2 mol/L) was added into it drop by drop with magnetic stirring for 30 min. Then, the white precipitation was centrifuged, washed, and dried in an oven (60 °C) for 24 h. The obtained sample was named as ZnO(S3). 50 mL of Cu(CH₃COO)₂ (0.5 mol/L) and 25 mL of glucose (1 mol/L) were mixed with a water bath (60 °C). After 10 min of magnetic stirring, 25 mL of NaOH solution (2 mol/L) was added into the mixture drop by drop with a continuous stirring. 30 min later, the brick red precipitation was centrifuged, washed, and dried under vacuum. Then, it was collected and named as Cu₂O(S4).

Characterization

The crystal structure was characterized using an X-ray powder diffractometer (XRD, TD-3500). The morphology and elemental mapping of the samples were examined using scanning electron microscope (SEM, SU1510; ZEISS Sigma 360) coupled with an energy dispersive spectrometer (EDS). The X-ray photoelectron spectroscopy (XPS) was analyzed by Thermo Scientific K-Alpha spectrometer. The specific surface area was measured by Automated Surface Area and Porosimetry Analyzer (Micromeritics ASAP 2460). The UV-Vis-DRS absorption spectra were performed using spectrometer (U3900).

Photocatalytic degradation of MB

Using methylene blue (MB) as a model organic pollutant and a xenon lamp as a simulated sunlight source, photocatalytic degradation experiments were carried out according to the procedure detailed in Ref. 6. In short, 150 mg of photocatalysts were put into MB solution (150 mL, 2.0×10⁻⁵ mol/L) with magnetic stirring continuously for 1 h in dark environment. After that, the mixed solution was irradiated by a xenon lamp with the light intensity of 100 mW/cm². The distance of lamp and solution was 15 cm. The degradation solution (1 mL) was taken out every 20 minutes and centrifuged in the dark. The absorbance of supernatant was monitored by an UV-Vis spectrophotometer in the wavelength range of 550 ~ 750 nm. The total illumination time was 100 min. The degradation ratio *R* was calculated according to the equation (1). In which, *A*₀ and *A*_t represent the initial and time-dependent absorbance of MB at 664 nm, respectively.

$$R(\%) = \frac{A_0 - A_t}{A_0} \times 100\% \quad (1)$$

RESULTS AND DISCUSSION

Material characterizations

The XRD patterns of the four samples were shown in Fig.1. For comparison, the standard powder diffraction files of Cu_2O with cubic crystal structure (PDF#65-3288) and ZnO with hexagonal wurtzite structure (PDF#36-1451) were also presented. Fig. 1a was the XRD pattern of S4 sample. The diffraction peaks (marked with *) matched well with those of cubic Cu_2O (PDF#65-3288), indicating that sample S4 was Cu_2O with cubic crystal structure. The XRD pattern of sample S3 was displayed in Fig. 1b. Comparison with the standard powder diffraction file for hexagonal wurtzite ZnO (PDF#36-1451) indicated that the diffraction peaks (marked with ♦) corresponded to hexagonal wurtzite ZnO in sample S3.

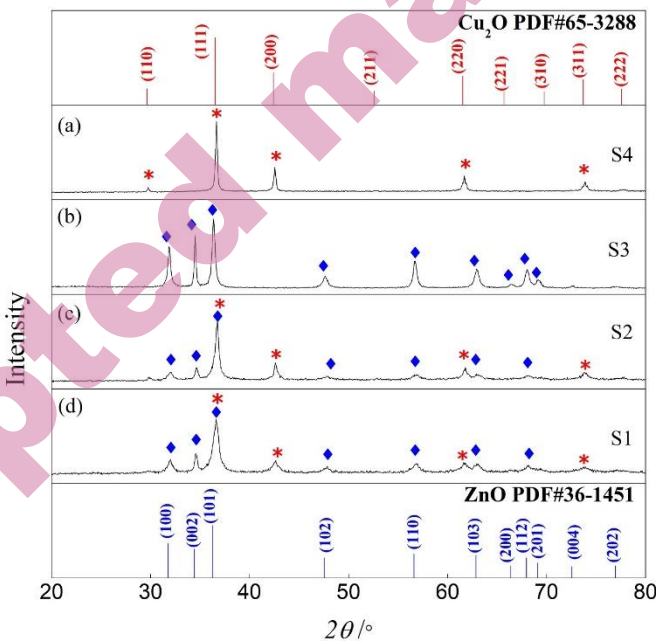


Fig. 1 The XRD patterns of samples: S4(a), S3(b), S2(c) and S1(d).

Figs.1d-c were the XRD patterns of S1 and S2 samples. The characteristic diffraction peaks (marked with ♦) corresponded to the (100), (002), (101), (102), (110), (103), and (112) crystal planes of ZnO with wurtzite structure, respectively. At the same time, the peaks at $2\theta=36.6^\circ$, 42.5° , 61.6° , and 73.9° (marked with *) matched with (111), (200), (220), and (311) crystal planes of cubic Cu_2O . These evidences confirmed that the samples of S1 and S2 were the composite of $\text{ZnO}/\text{Cu}_2\text{O}$. Moreover, the crystal structure of the component was unchanged under the mediation of SDS. In addition, there was no other diffraction peaks in Figs. 1a-

d, and the sharp peaks declared the synthesized samples were with good crystallinity.

Fig. 2 was the XPS spectra of the ZnO/Cu₂O (S1) composite. The survey spectrum (Fig. 2a) indicated that Zn, O and Cu elements were existed in the composite. In the line spectrum of Zn 2p (Fig. 2b), there existed two dominant peaks at 1021.8 eV and 1044.7 eV, which was attributed to the Zn 2p_{3/2} and Zn 2p_{1/2} of Zn²⁺ respectively.²⁴ In the XPS data of O 1s (Fig. 2c), the first peak located at 530.4 eV, corresponding the lattice oxygen in ZnO and Cu₂O,^{13,25} the second peak appeared at the binding energy of 531.7 eV might be attributed to hydration.²⁵⁻²⁶ As shown in Fig. 2d, two binding energy peaks of Cu 2p were observed at 932.4 eV and 952.3 eV, which were ascribed to those of Cu 2p_{3/2} and Cu 2p_{1/2} from Cu⁺ in Cu₂O, respectively.^{13,27-28} In addition, two satellite peaks located at 942.3 eV and 962.1 eV of Cu(II) were identified, indicating the existence of CuO.²⁹ However, it was worth mentioning that no characteristic peaks of CuO were detected in the XRD pattern of sample S1, demonstrating that only few Cu₂O were oxidized to CuO on the surface of the composite. It might be due to the surface sensitivity of the XPS characterization technique. In summary, the characterization of XPS demonstrated the successful synthesis of ZnO/Cu₂O (S1) composite.

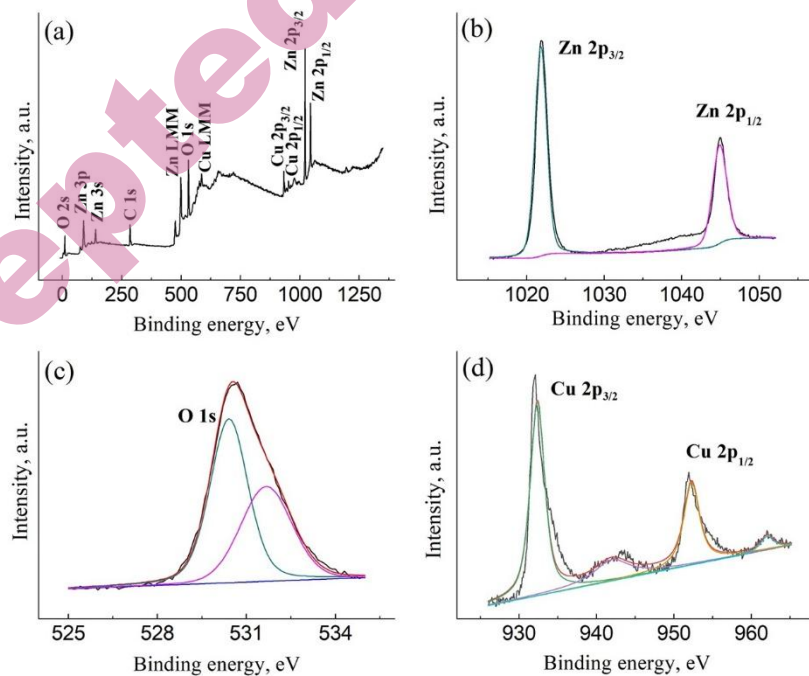


Fig. 2 The XPS spectra of ZnO/Cu₂O(S1): survey spectrum (a), Zn 2p (b), O 1s (c), Cu 2p (d).

Fig. 3 revealed the SEM images of ZnO, Cu₂O, ZnO/Cu₂O(S2), ZnO/Cu₂O(S1), together with the EDS spectra and elemental mapping images of ZnO/Cu₂O(S1). It can be observed that the morphologies of ZnO particles were irregular, which sizes were in the range of 0.2~1 μ m (Fig.3a). Cu₂O particles, ranging from 0.5 to 2.5 μ m, exhibited polyhedral or spherical shapes with smooth surfaces (Fig.3b). For ZnO/Cu₂O(S2) composite (Fig.3c), it could be seen that ZnO particles adhered to the surface of Cu₂O, in which, the morphology and size of Cu₂O particles showed little change compared to the pure Cu₂O particles (Fig.3b). Figs.3d-f displayed that the composite of ZnO/Cu₂O(S1) was consisted of nano-spherical Cu₂O aggregates and flower-like ZnO particles. The aggregates of Cu₂O were formed by the self-assembly of Cu₂O particles with a size of 50~100 nm. The size of nano-spherical Cu₂O aggregates was obviously smaller than that of Cu₂O shown in Fig.3b. Moreover, the size and morphologies of ZnO particles underwent significant changes comparing with pure ZnO (Fig.3a). Through Figs.3d-f, it could be found that the particle size of ZnO with flower morphology was about 200 nm.

From the EDS spectra (Figs. 3g-h), the elements of Cu, Zn, and O were detected, and no other additional elements were found, which confirmed the composition of ZnO/Cu₂O(S1) composite. Additionally, it could be seen that Cu, Zn, and O elements (Figs. 3i-k) were uniformly distributed which further verified the successful synthesis of ZnO/Cu₂O(S1) composite with high purity.

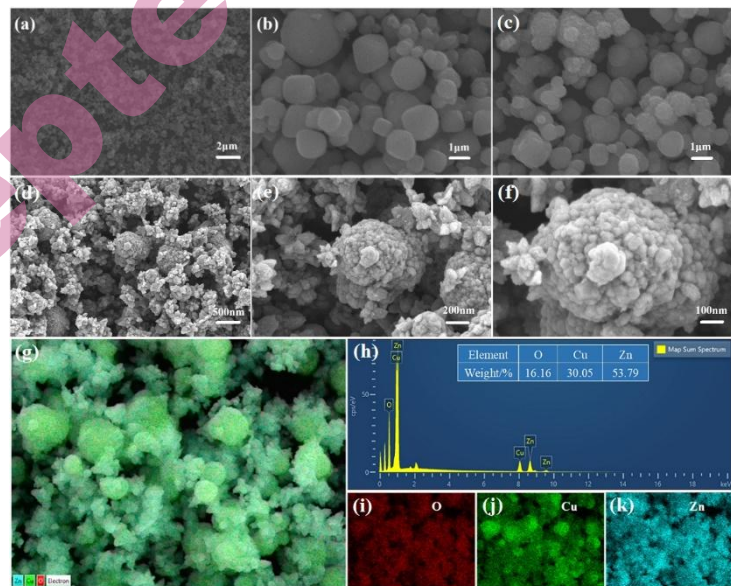


Fig. 3 SEM images of ZnO (a), Cu₂O (b), ZnO/Cu₂O(S2) (c), ZnO/Cu₂O(S1) (d-f), EDS spectra (g-h) and elemental mapping images (i-k) of ZnO/Cu₂O(S1)

The change of particle size and morphology of ZnO/Cu₂O(S1) composite was closely related to the regulation of SDS. As a surfactant, the molecules of SDS could form self-assembly aggregates with unique spatial structure when its concentration reached a specific value. These aggregates with obvious structural interfaces could act as soft template to induce the formation of the materials with specific structures, morphologies, and properties. The hydrophilic group of SDS were negatively charged and attracted Zn²⁺ and Cu²⁺ ions to gather around them by electrostatic attraction.³⁰⁻³¹ Then, the distributions of metal cations in the solution were changed, and the crystal nucleation sites were regulated. Due to the template effect, the crystal underwent a controlled growth. The structure and morphology of the obtained sample were shaped and the desired property was endowed.

Fig. 4a displayed the N₂ adsorption–desorption isotherm of ZnO/Cu₂O(S1) composite. The curve accorded with typical type IV isotherm and displayed an obvious hysteresis loop of type H3, indicating the presence of a large number of mesopores.³² The specific surface area measured by BET method was 17.15 m²/g. The pore size distribution calculated by BJH method was shown in Fig. 4b. The average pore diameter was 11.98 nm. The mesoporous channels can facilitate the diffusion of reactant molecules into the interior of the material, which endow the composite with the advantage of adsorption for pollutants and then enhance its photocatalytic performance.

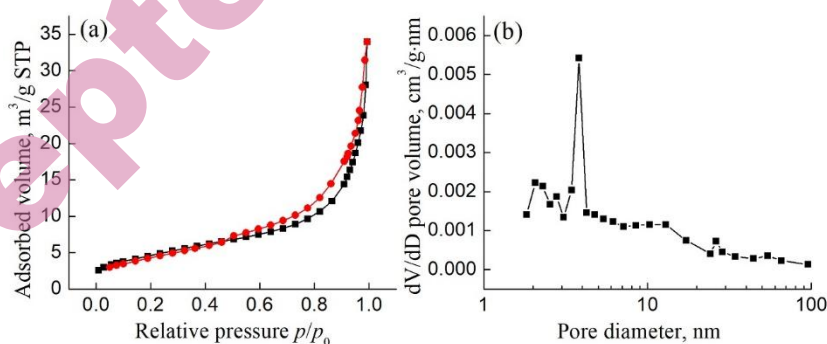


Fig. 4 N₂ adsorption-desorption isotherm (a) and pore size distribution (b) of ZnO/Cu₂O(S1)

Fig. 5a showed the UV-Vis-DRS absorption spectra of ZnO, Cu₂O and ZnO/Cu₂O(S1). It can be observed that ZnO/Cu₂O(S1) exhibited strong adsorption in the region from 400 to 800 nm. Comparing with ZnO, the photo-response range expanded to the visible region. According to the Kubelka-Munk transformation and Tauc formulas,³³⁻³⁵ the band gap energies (E_g) of ZnO, Cu₂O and ZnO/Cu₂O(S1) were calculated and displayed in Fig. 5b. the E_g value of Cu₂O and ZnO were approximately 1.99 and 3.25 eV, respectively, which were basically

consistent with previous reports.^{27,32} Two E_g values of 2.06 eV and 3.22 eV existed for ZnO/Cu₂O(S1) composite. The E_g value of Cu₂O in the composite was 2.06 eV, which was larger than that of pure Cu₂O (1.99 eV), it lowered the recombination rate of e^-/h^+ .³³ At the same time, the E_g value of ZnO in the composite was 3.22 eV, instead of 3.25 eV of pure ZnO, the narrowing of the band gap induced the red-shift of the absorption edge.³² The changes of band gap energy were attributed to successful incorporation of ZnO and Cu₂O in the composite, which resulting in the enhancement of photocatalytic properties.

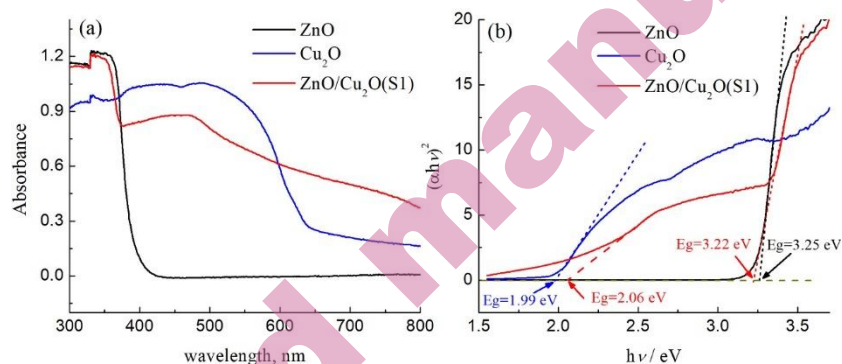


Fig. 5 The UV-Vis-DRS absorption spectra (a) and Tauc plot (b) to calculate the band gap energy

Photocatalytic activity and stability analysis

Fig. 6 presented the UV-Vis spectra of MB solution which underwent photocatalytic degradation by the photocatalysts of ZnO/Cu₂O(S1), ZnO/Cu₂O(S2), ZnO, and Cu₂O after different times, respectively. The absorbance values of the solution decreased at the wavelength of 664 nm (the maximum absorption peak of MB³⁶⁻³⁸) with the elapse of illumination time, which suggested that MB was degraded gradually.

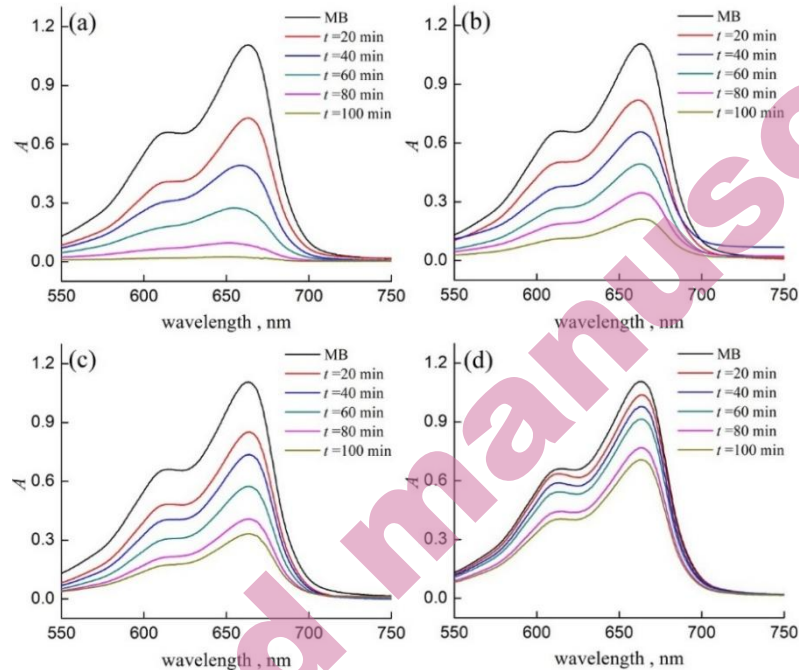


Fig. 6 The UV-Vis spectra of MB solution degraded by ZnO/Cu₂O(S1) (a), ZnO/Cu₂O(S2) (b), ZnO(c), and Cu₂O(d)

To present the photocatalytic performance more intuitively, the degradation ratio R was calculated and shown in Fig. 7a. The results showed the relationship of R : $R(\text{ZnO/Cu}_2\text{O(S1)}) > R(\text{ZnO/Cu}_2\text{O(S2)}) > R(\text{ZnO}) > R(\text{Cu}_2\text{O})$. Taking 100 min as an example, the degradation ratio R of MB by ZnO/Cu₂O(S1) reached 98.1%, while R of MB by ZnO/Cu₂O(S2), ZnO, and Cu₂O were only 80.8%, 70.0% and 36.0%, respectively. Therefore, the photocatalytic efficiency of ZnO/Cu₂O(S1) was the best among the four photocatalysts.

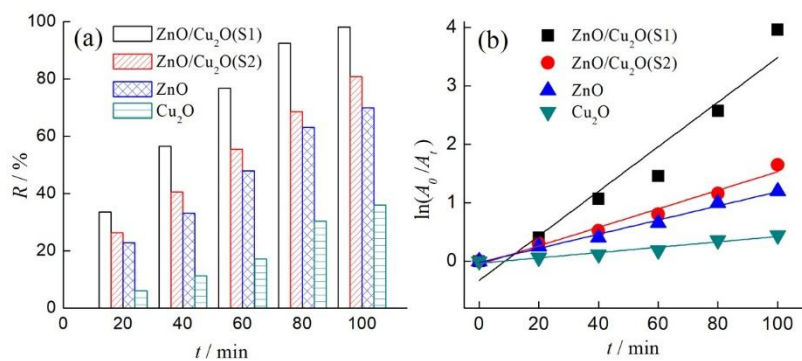


Fig. 7 $R \sim t$ histogram (a) and the kinetic curves (b) of photocatalytic degradation of MB

In order to evaluate the degradation kinetics of MB by the synthesized photocatalysts, the curves of $\ln(A_0/A_t) \sim t$ were plotted and shown in Fig.7b. There was a good linear relationship between $\ln(A_0/A_t)$ and the time of t , which accorded with the kinetic characteristics of pseudo first-order. The kinetic parameters of the fitting curves were summarized in Table I. From the data, it was demonstrated that the k value of the degradation reaction using ZnO/Cu₂O(S1) as the photocatalyst was about 2.4, 3.2, and 8.3 times that of ZnO/Cu₂O(S2), ZnO, and Cu₂O, respectively. Therefore, the ZnO/Cu₂O(S1) nanocomposite presented an ideal degradation efficiency under the same conditions, demonstrating promising potentiality for photocatalytic applications.

TABLE I. Parameters of kinetic curves

Sample	Rate constant k/min^{-1}	R^2
ZnO/Cu ₂ O(S1)	0.03814	0.92797
ZnO/Cu ₂ O(S2)	0.01585	0.97676
ZnO	0.01210	0.98707
Cu ₂ O	0.00457	0.94903

The enhanced photocatalytic performance of ZnO/Cu₂O(S1) maybe attributed to the mediation of SDS and the synergistic effect of ZnO and Cu₂O components in the composite. The results of SEM suggested that the morphology of both ZnO and Cu₂O changed obviously in shape and the size of them became smaller. The BET characterization revealed that the average pore diameter was 11.98nm. The changes of morphology and particle size, as well as the abundant presence of mesopores in the composite were closely related to the template effect of SDS. It might make it easier to contact with the molecules of MB and offer more surface adsorption sites, and then facilitated the further occurrence of oxidative decomposition. In addition, another important factor could not be ignored. The energy level matching of Cu₂O and ZnO in the composite promoted the separation of photo-generated charge carriers-electron(e^-)/hole(h^+) pairs,^{17,33,38} and then improved its catalytic ability. The possible mechanism was described,^{17,23,33,39} and the corresponding mechanism diagram was shown in Fig.8. The e^- in the valence band (VB) of Cu₂O and ZnO transferred to the conduction band (CB) under the irradiation of light, and the h^+ was left in the VB. Because the CB position of Cu₂O is higher than that of ZnO, the photo-generated e^- in the CB of Cu₂O transferred to the surface of ZnO; at the same time, the h^+ in the VB of ZnO transferred to the surface of Cu₂O, thus effectively avoiding the recombination of e^- and h^+ on the catalyst surface. h^+ and e^- with strong oxidation and reduction ability react with H₂O and O₂, respectively, to form reactive hydroxide radicals ($\cdot\text{OH}$) and super oxide radical anion ($\cdot\text{O}_2^-$), in which, $\cdot\text{O}_2^-$ can further turn into $\cdot\text{OH}$.^{13,24,27,33,39} The $\cdot\text{OH}$ has perfect oxidation ability to degrade MB molecules into CO₂ and H₂O.

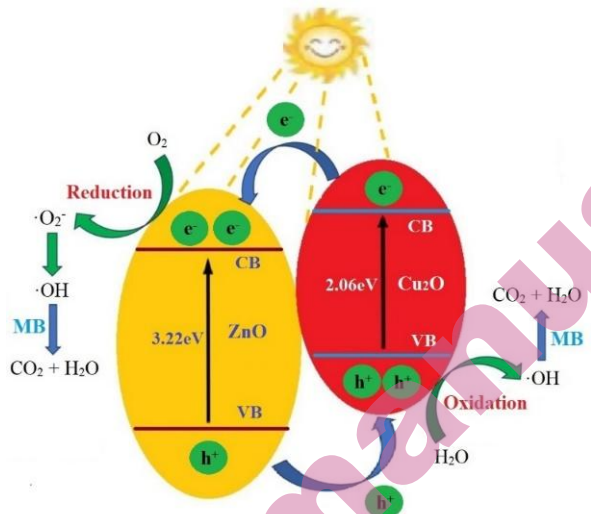


Fig. 8 Possible mechanism of photocatalytic degradation of MB by ZnO/Cu₂O(S1)

The stability of ZnO/Cu₂O(S1) was tested by recycling the sample in the photocatalytic degradation experiment of MB. As shown in Fig. 9, after 5 times cycling of photocatalytic degradation, R only decreased from 98.1% to 92.1%, indicating that ZnO/Cu₂O(S1) has good photocatalytic stability.

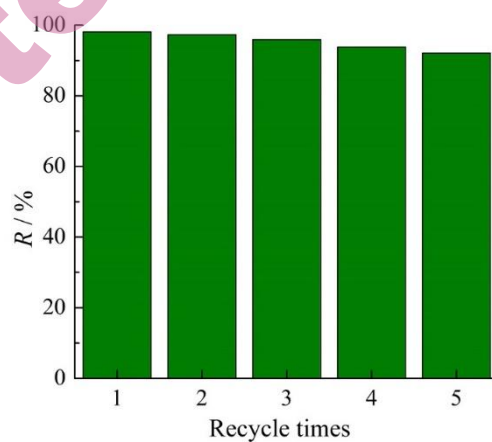


Fig. 9 Recycling experiments of ZnO/Cu₂O(S1) composite

CONCLUSION

In summary, ZnO/Cu₂O(S1) nanocomposite was prepared by one-pot method. During the process of preparation, SDS served an effective template. The characterizations confirmed that flower-like ZnO nanoparticles (hexagonal

wurtzite) grew on the Cu₂O nanospheres (cubic crystal) self-assembled from single Cu₂O particles, and Cu, Zn, and O elements were uniformly distributed in the composite. Abundant mesopores were existed in ZnO/Cu₂O(S1) and the photo-response range expanded to the visible region. The photocatalytic degradation tests indicated that the degradation ratio R of MB by ZnO/Cu₂O(S1) reached 98.1% after 100 min illumination, significantly larger than that of ZnO (70.0%), Cu₂O (36.0%), and ZnO/Cu₂O(S2) (80.8%), and R did not obviously decrease after 5 recycling, demonstrating high photocatalytic degradation ability and good photocatalytic stability. The enhanced photocatalytic property maybe attributed to the inducement of SDS and the synergy effect of ZnO and Cu₂O. The advantages of smaller particle sizes, larger amount of mesopores, more surface adsorption sites, stronger absorption in the visible light range and easier separation of photo-generated carriers (e⁻/h⁺) will help to improve its catalytic degradation ability. The ZnO/Cu₂O nanocomposite assisted by SDS shows a good application prospect for sewage treatment.

Acknowledgements: This work is supported by Anhui Province Young Teacher Training Action: Discipline (Major) Leader Cultivation Project (DTR2023037), Anhui Provincial Teaching Innovation Team (2023cxtd073), Natural Science Foundation of the Department of Education of Anhui Province (2025AHGXZK31414, 2022AH052139), Anhui Engineering Laboratory for Medicinal and Food Homologous Natural Resources Exploration (2025KYPT04) and National/Provincial College Students Innovation Training (202514098035/S202514098176). The authors extend their gratitude to Mr. Yangjin Zhang (from Scientific Compass www.shiyanjia.com) for providing invaluable assistance with the SEM, XPS and BET analysis.

И З В О Д

ПОБОЉШАНА ФОТОКАТАЛИТИЧКА АКТИВНОСТ ZnO/Cu₂O КОМПОЗИТА ЗА РАЗГРАДЊУ МЕТИЛЕН ПЛАВОГ УСЛЕД СИНЕРГИСТИЧКОГ ЕФЕКТА

HONGYING LI,^{1,2} LUWEN MA,¹ ZHENYANG WU¹ И CHENGLI YAO¹

¹School of Chemistry and Pharmaceutical Engineering, Hefei Normal University, Hefei, Anhui, China и ²Hefei National Research Center for Physical Sciences at the Microscale, University of Science and Technology of China, Hefei, Anhui, China.

У циљу испитивања катализитичке ефикасности разградње ZnO/Cu₂O композита, синтетисан је нанокомпозит применом „опе-рот“ методе и SDS једињења. Кристална структура, микроскопска морфологија, хемијски састав, специфична површина, расподела величине пора и оптичка апсорпциона својства композита су детаљно окарактерисани. Испитивана је фотокатализитичка активност композита према разградњи метилен плавог (MB) у присуству зрачења ксенонске лампе. Резултати карактеризације су показали да се синтетисани композит састоји од ZnO (хексагонална вурцитна структура) и Cu₂O (кубна кристална структура). Захваљујући посредовању SDS једињења, добијене честице су нанометарских димензија, са равномерном расподелом елемената Cu, Zn и O, као и са великим бројем мезопора. Опсег фотокатализитичке активности композита је проширен на видљиви део спектра услед комбинације ZnO и Cu₂O. Степен разградње MB једињења у

присуству ZnO/Cu₂O композита износио је приближно 92% за 100 min и након пет циклуса поновне примене, што указује на значајан потенцијал за фотокаталитичке примене. Побољшана фотокаталитичка активност може бити повезана са посредовањем SDS једињења током процеса припреме и синергистичким ефектом између ZnO и Cu₂O.

(Примљено 15. новембра 2025; ревидирано 27. новембра 2025; прихваћено 29. јануара 2026.)

REFERENCES

1. C. Ashina, N. Pugazhenthiran, R. V. Mangalaraja, P. Sathishkumar, *Renew. Sust. Energ. Rev.* **214** (2025) 115490 (<https://doi.org/10.1016/j.rser.2025.115490>)
2. C. Vanlalhmingmawia, H. Moradi, Y. J. Kim, D. S. Kim, J. K. Yang, *Chem. Eng. J.* **509** (2025) 161335 (<https://doi.org/10.1016/j.cej.2025.161335>)
3. C. Q. Shen, X. Y. Li, B. Xue, D. J. Feng, Y. P. Liu, F. Yang, M. Y. Zhang, S. J. Li, *Appl. Surf. Sci.* **679** (2025) 161303 (<https://doi.org/10.1016/j.apsusc.2024.161303>)
4. H. Tu, B. H. Tian, Z. C. Zhao, R. J. Guo, Y. Wang, S. H. Chen, J. Wu, *Water Res. X* **28** (2025) 100315 (<https://doi.org/10.1016/j.wroa.2025.100315>)
5. M. Y. Areeshi, *Luminescence* **38** (2023) 1111 (<https://doi.org/10.1002/bio.4432>)
6. H. Y. Li, X. X. Liu, J. Q. Huang, W. J. Zhu, A. M. Ding, C. L. Yao, J. M. Zhu, *Crystallogr. Rep.* **67** (2022) 1231 (<https://doi.org/10.1134/S1063774522070082>)
7. H. Zhao, Z. H. Zhan, W. C. Li, N. Zhang, X. Ma, P. K. Yan, Y. J. Gao, H. L. Cong, Q. Zhang, *J. Alloy. Compd.* **1002** (2024) 175197 (<https://doi.org/10.1016/j.jallcom.2024.175197>)
8. L. Nadja, A. Chakib, K. Mohamed, T. Mohamed, E. Abdelkader, *Appl. Phys. A-Mater.* **131** (2025) 154 (<https://doi.org/10.1007/s00339-024-08223-x>)
9. D. Xu, H. L. Ma, *J. Clean. Prod.* **313** (2021) 127758 (<https://doi.org/10.1016/j.jclepro.2021.127758>)
10. A. L. Yang, L. L. Wang, *Curr. Nanosci.* **18** (2022) 94 (<https://doi.org/10.2174/1573413717666210129115305>)
11. R. Rathinabala, R. Thamizselvi, D. Padmanabhan, S. F. Alshahateet, I. Fatimah, A. K. Sibhatu, G. K. Weldegebrreal, S. I. A. Razak, S. Sagadevan, *Inorg. Chem. Commun.* **143** (2022) 109783 (<https://doi.org/10.1016/j.inoche.2022.109783>)
12. P. Attri, S. Garg, J. K. Ratan, A. S. Giri, *Korean J. Chem. Eng.* **41** (2024) 3191 (<https://doi.org/10.1007/s11814-024-00283-2>)
13. J. K. Nie, X. J. Yu, Z. B. Liu, J. Zhang, Y. Ma, Y. Y. Chen, Q. G. Ji, N. N. Zhao, Z. Chang, *J. Clean. Prod.* **363** (2022) 132593 (<https://doi.org/10.1016/j.jclepro.2022.132593>)
14. T. Bekele, G. Mebratие, A. Girma, G. Alamnie, *Colloids and Surfaces A.*
15. X. J. Yu, Z. Y. Li, Z. B. Liu, K. Wang, *Appl. Surf. Sci.* **665** (2024) 160285 (<https://doi.org/10.1016/j.apsusc.2024.160285>)
16. P. Liang, W. Y. Yang, H. Y. Peng, S. H. Zhao, *Molecules* **29** (2024) 5584 (<https://doi.org/10.3390/molecules29235584>)
17. X. S. Wang, Y. D. Zhang, Q. C. Wang, B. Dong, Y. J. Wang, W. Feng, *Sci. Eng. Compos. Mater.* **26** (2019) 104 (<https://doi.org/10.1515/secm-2018-0170>)
18. X. S. Jiang, Q. B. Lin, M. Zhang, G. He, Z. Q. Sun, *Nanoscale Res. Lett.* **10** (2015) 30 (<https://doi.org/10.1186/s11671-015-0755-0>)
19. C. L. Yao, C. Chen, Y. J. Yuan, W. J. Zhu, W. Q. Tai, C. Ding, H. Y. Li, *Cryst. Res. Technol.* **59** (2024) 2300233 (<https://doi.org/10.1002/crat.202300233>)

20. M. Amano, K. Hashimoto, H. Shibata, *J. Oleo. Sci.* **71** (2022) 927 (<https://doi.org/10.5650/jos.ess22061>)

21. J. Cui, L. Ye, X. X. Chen, J. N. Li, B. Yang, M. Yang, Q. Yang, D. Q. Yun, S. D. Sun, *Appl. Surf. Sci.* **638** (2023) 158046 (<https://doi.org/10.1016/j.apsusc.2023.158046>)

22. A. Norouzi, A. Nezamzadeh-Ejhieh, *Mater. Res. Bull.* **164** (2023) 112237 (<https://doi.org/10.1016/j.materresbull.2023.112237>)

23. K. Chitalkar, D. Hase, S. Gurav, S. Musmade, R. Gaikar, M. Sillanpää, V. Murade, H. Aher, *J. Inorg. Organomet. Polym.* **35** (2025) 6961 (<https://doi.org/10.1007/s10904-025-03705-8>)

24. X. J. Yu, J. Zhang, J. Zhang, J. F. Niu, J. Zhao, Y. C. Wei, B. H. Yao, *Chem. Eng. J.* **374** (2019) 316 (<https://doi.org/10.1016/j.cej.2019.05.177>)

25. F. Liu, Y. L. Che, Q. W. Chai, M. F. Zhao, Y. Lv, H. Sun, Y. Q. Wang, J. Sun, C. C. Zhao, *Environ. Sci. Pollut. R.* **26** (2019) 25286 (<https://doi.org/10.1007/s11356-019-05814-7>)

26. Y. W. Lu, F. Yu, J. Hu, J. Liu, *Appl Catal A-Gen* **429** (2012) 48 (<https://doi.org/10.1016/j.apcata.2012.04.005>)

27. J. K. Nie, X. J. Yu, Z. B. Liu, Y. C. Wei, J. Zhang, N. N. Zhao, Z. Yu, B. H. Yao, *Appl. Surf. Sci.* **576** (2022) 151842 (<https://doi.org/10.1016/j.apsusc.2021.151842>)

28. J. K. Nie, X. J. Yu, Y. C. Wei, Z. B. Liu, J. Zhang, Z. Yu, Y. Ma, B. H. Yao, *Process Saf. Environ.* **170** (2023) 241 (<https://doi.org/10.1016/j.psep.2022.12.002>)

29. T. Nesavi · L. Balu · R. Ezhil Pavai, *Ionics* **31** (2025) 12027 (<https://doi.org/10.1007/s11581-025-06697-0>)

30. J. H. Cao, L. P. Ding, W. T. Hu, X. L. Chen, X. Chen, Y. Fang, *Langmuir* **30** (2014) 15364 (<https://doi.org/10.1021/la5039798>)

31. C. L. Yao, A. J. Xie, Y. H. Shen, W. N. Zhu, J. M. Zhu, *Cryst. Res. Technol.* **49** (2014) 982 (<https://doi.org/10.1002/crat.201400300>)

32. Y. F. Wang, J. Gao, X. Z. Wang, L. P. Jin, L. L. Fang, M. Zhang, G. He, Z. Q. Sun, *J. Sol-Gel Sci. Techn.* **88** (2018) 172 (<https://doi.org/10.1007/s10971-018-4786-8>)

33. N. Akter, T. Ahmed, I. Haque, M. K. Hossain, G. Ray, M. M. Hossain, M. S. Islam, M. A. A. shaikh, U. S. Akhtar, *Helijon* **10** (2024) e30802 (<https://doi.org/10.1016/j.helijon.2024.e30802>)

34. Z. B. Liu, X. J. Yu, K. Wang, J. Zhang, J. F. Niu, *Sep. Purif. Technol.* **356** (2025) 129810 (<https://doi.org/10.1016/j.seppur.2024.129810>)

35. B. Simović, Ž. Radovanović, G. Branković, A. Dapčević, *Mat. Sci. Semicon. Proc.* **162** (2023) 107542 (<https://doi.org/10.1016/j.mssp.2023.107542>)

36. X. J. Yu, J. Zhang, Y. Y. Chen, Q. G. Ji, Y. C. Wei, J. F. Niu, Z. Yu, B. H. Yao, *J. Environ. Chem. Eng.* **9** (2021) 106161 (<https://doi.org/10.1016/j.jece.2021.106161>)

37. H. Usui, *J. Colloid Interf. Sci.* **336** (2009) 667 (<https://doi.org/10.1016/j.jcis.2009.04.060>)

38. X. J. Yu, Q. G. Ji, Y. C. Wei, Z. B. Liu, N. N. Zhao, M. Yang, Q. Yang, *J. Electrochem. Soc.* **168** (2021) 126513 (<https://doi.org/10.1149/1945-7111/ac3e79>)

39. S. Y. Gao, J. J. Zhang, W. Q. Li, S. J. Jiao, Y. G. Nie, H. Y. Fan, Z. Zeng, Q. J. Yu, J. Z. Wang, X. T. Zhang, *Chem. Phys. Lett.* **692** (2018) 14 (<https://doi.org/10.1016/j.cplett.2017.11.062>).